Electrochemical Characteristics of Nanotube Formed Ti-Zr Alloy

W.G.Kim, *H.C. Choe, Y.M. Ko, [1]W. A. Brantley

College of Dentistry, Chosun University, 2nd stage of Brain Korea 21 for College of Dentistry, Gwangju, Korea
[1]College of Dentistry, Ohio State University, Columbus, OH, USA
*hcchoe@chosun.ac.kr

ABSTRACT

In this paper, Ti-Zr(10, 20, 30 and 40 wt%) alloys were prepared by arc melting and nano-structure controlled for 24 hr at 1000 °C in argon atmosphere. Formation of oxide nanotubes are conducted by anodizing a Ti-Zr alloy in H_3PO_4 electrolytes with small amounts of fluoride ions at room temperature. The corrosion properties of the specimens were examined through potentiodynamic test (potential range of -1500 ~ 2000 mV) in 0.9% NaCl solution by potentiostat (EG&G Co, PARSTAT 2273. USA). Microstructures of the alloys were examined by optical microscopy (OM), scanning electron microscopy (SEM) and X-ray diffractometer (XRD). Diameter of nanotube was not depended on Zr content, but interspace of nanotube was predominantly depended on Zr content. It is confirmed that, ZrO_2 oxides play a role to formation on the surface.

Keywords: Nano-structure, Corrosion, Ti-Zr alloy, dental implant

1 INTRODUCTION

Titanium alloys are expected to be much more widely used for implant materials in the medical and dental fields because of their superior biocompatibility, corrosion resistance and specific strength compared with other metallic implant materials. The use of titanium and its alloys implant applications has mainly been limited to the alloy Ti-6Al-4V and to CP-Ti [1,2]. For medical application titanium and Ti-6Al-4V have been used since 1960s, with Ti-6Al-4V gradually replacing CP-Ti due to the increased mechanical strength of plates, nails, screws and endoprostheses [3].

Recently, however, much concern has developed over the issue of biocompatibility with respect to the dissolution of aluminum and vanadium ions and the possibility of any toxic effects [4-6]. Consequently, other titanium alloys are currently being considered as alternatives to the Ti-6Al-4V alloy. Therefore, Ti-alloy, Al and V free and composed of non-toxic element such as Nb and Zr as biomaterials have been developed. Especially, Zr element belongs to same family in periodic table as Ti element. Addition of Zr to Ti alloy has an excellent mechanical properties, good corrosion resistance and biocompatibility [7].

The high degree of biocompatibility of Ti alloys is usually ascribed to their ability to form stable and dense oxide layers consisting mainly of TiO_2. The native oxide layers on Ti are usually 2-5nm thick and are spontaneously rebuilt in most environments whenever they are mechanically damaged. It is believed that thicker and more stable TiO_2 based oxide surfaces are generally favorable for surface bioactivity [8,9]. Spark anodization is one of the conventional routes to increase the biocompatibility of titanium and its alloys. This process typically leads to the formation of a disordered oxide structure (irregular pores with lateral features from 1 to 10㎛) several hundreds of nanometers thick [10,11]. In contrast to this approach, the electrochemical formation of novel highly ordered oxide nanotube layers has been reported for Ti anodization in fluoride containing acid electrolytes at moderate voltages [12]. Such TiO_2 structures consist of arrays of nanotubes with diameters in the 100 nm range and thickness up to about 400~500 nm.

In order to investigate the electrochemical characteristics of nanotube formed Ti-xZr alloy for biomaterials have been researched using by electrochemical methods.

2 MATERIALS AND METHODS

2.1 Alloy preparation

Ti (G&S TITANIUM, Grade. 4, USA)alloys containing Zr(Kurt J. Lesker Company, 99.95 % wt% in purity) up to 10,20, 30 and 40 wt% were melted six times to improve chemical homogeneity using the vacuum arc melting furnace. And heat treatment was carried out at 1000℃ for 24h in order to homogenization in argon atmosphere.

The specimens for electrochemical test were prepared by using various grit emery papers and then finally, polished with 0.3 ㎛ Al_2O_3 powder. All of polished specimen was ultrasonically cleaned and degreased in acetone.

2.2 Microstructure analysis

Microstructures of the alloys were examined by optical microscopy (OM, OLYMPUS BM60M, JAPAN) and

NSTI-Nanotech 2008, www.nsti.org, ISBN 978-1-4200-8503-7 Vol. 1

scanning electron microscopy (SEM, HITACHI-3000, JAPAN). The specimens for the OM and SEM analysis were etched in Keller's solution consisting of 2 ㎖ HF, 3 ㎖ HCl, 5 ㎖ HNO_3 and 190 ㎖ H_2O.

In order to identify the phase constitutions of the Ti-xZr alloys, X-ray diffractometer (XRD, Philips, X'pert Pro MPD) analysis with a Cu-Kα radiation were performed.

2.3 Anodization test

Electrochemical experiments were carried out with conventional three-electrode configuration with a platinum counter electrode and a saturated calomel reference electrode. The sample was embedded with epoxy resin, leaving a square surface area of $10mm^2$ exposed to the anodizing electrolyte, 1M H_3PO_4 containing 0.5wt% NaF. Anodization treatments were carried out using a scanning potentiostat (EG&G Co., Model 362, USA). All experiments were conducted at room temperature. The electrochemical treatments consist of potential was first swept from the open-circuit potential to desired final potential with a sweep rate of 500mV/s, then the potential was held for 2h. After the treatments the anodized sample were rinsed with distilled water and dried with dry air stream.

2.4 Electrochemical test

The corrosion behaviors were investigated using potentiostat (EG&G Co, 2273A) in NaCl solution at 36.5 ± 1℃. A conventional three-electrode cell with a high dense carbon as counter electrode, saturated calomel (SCE) as reference electrode, and specimens as working electrode, connected to a potentiostat, was used to conduct the potentiodynamic test.

3 RESULT AND DISCUSSION

3.1 Microstructural observations

Fig. 1,2 shows the microstructures of Ti-xZr alloys with different Zr contents (10, 20, 30 and 40 wt.%). The microstructures of Ti-10Zr and Ti-20Zr alloy showed lamellar structure and needle-like structure, these phase changed gradually to almost needle-like structure in Ti-40Zr alloy. Consequently, microstructures of Ti-xZr alloys were changed from lamellar structures to needle-like structure as Zr content increased.

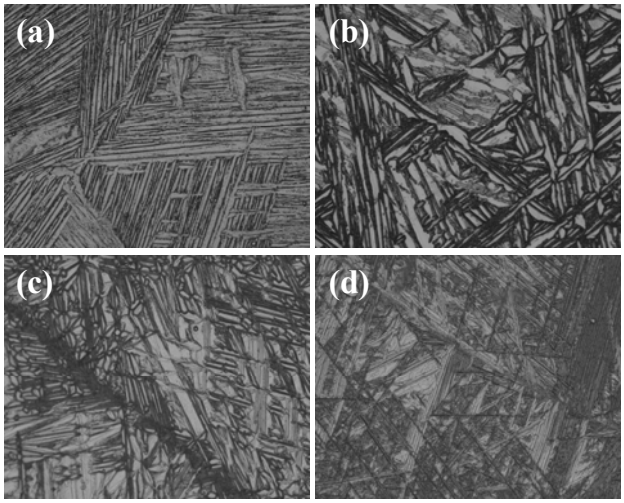

Fig. 1. OM micrographs of homogenized Ti-xZr alloys (a) Ti-10Zr (b) Ti-20Zr (c) Ti-30Zr (d) Ti-40Zr

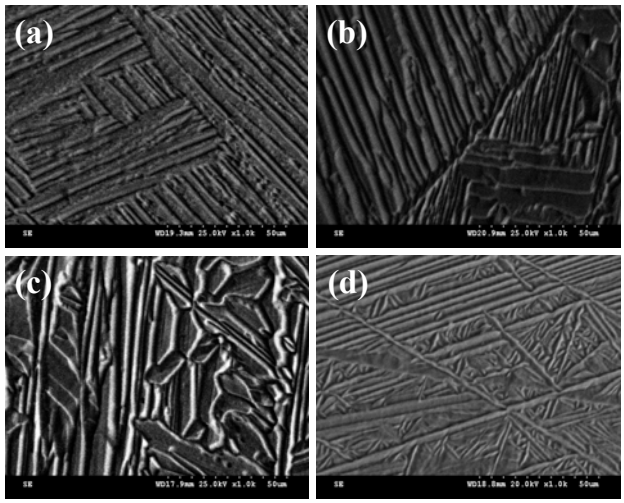

Fig. 2. SEM micrographs of homogenized Ti-xZr alloys (a) Ti-10Zr (b) Ti-20Zr (c) Ti-30Zr (d) Ti-40Zr

As a result of interpretation using software (Nwetown Square. JCPDS win, USA) for each peak, X-ray diffracto-meter (XRD) of the homogenized Ti-xZr alloys are summarized in Fig. 3, which indicate that the phase transformation in the Ti-xZr alloys sensitive to Zr content. It suggested that β → α transformation progressed gradually with increasing Zr content due to Zr displacement [13]. Each diffraction peak shifted to a lower angle with increasing Zr content. The absence of additional peaks is consistent with single-phase.

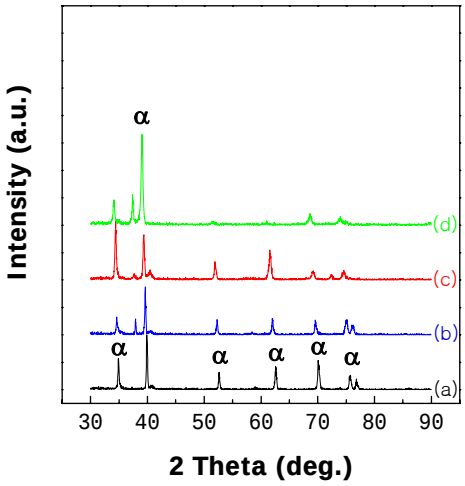

Fig. 3. X-ray diffracto-meter of Ti-xZr alloys
(a) Ti-10Zr (b) Ti-20Zr (c) Ti-30Zr (d) Ti-40Zr

3.2 Nanotube structures

The microstructures shown in Fig. 4 are taken from the Ti-20Zr, which were TiO_2 nanotube layer formed on Ti substrate. In the microstructures that are presented, beta phase appears dark area and the alpha phase shows the light area. The microstructure of Ti-20Zr, provided in Fig. 4, reveals elongated alpha/beta phase interface. Nanotube was formed mainly on the alpha phase with many tube like stacked ring. It is confirmed that number of ring is related to nanotube formation time and to the periodicity of current oscillations. In the alpha phase, shape of nanotube is different from that of beta phase.

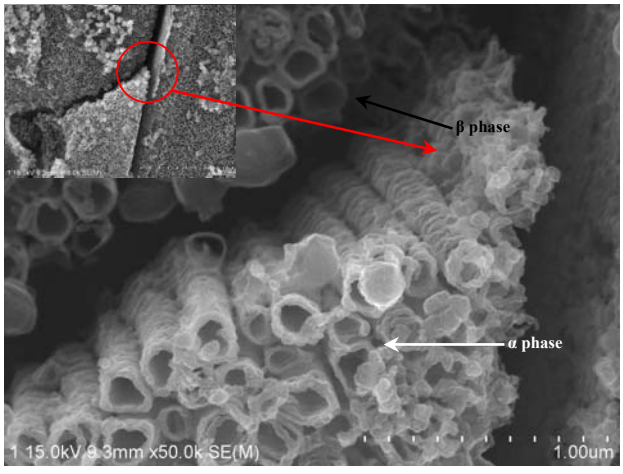

Fig. 4. SEM micrographs of TiO_2 nanotube layer formed Ti-20Zr alloy

Fig. 5 shows a typical SEM image of TiO_2 nanotube layer prepared by anodizaiton of titanium at 10V in 1M H_3PO_4 + 0.5wt% NaF for 2h. The nanotubes have an inner average diameter of 150 ~ 200 nm with a tube-wall thickness of about 20nm.

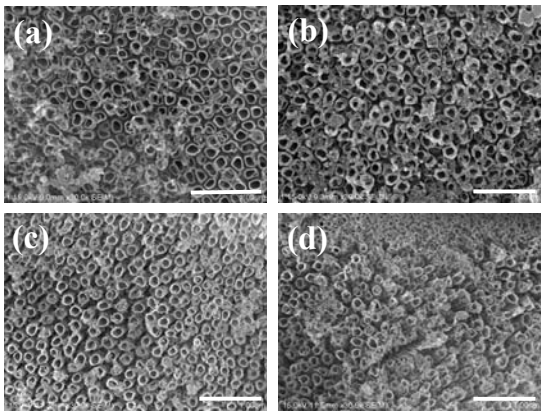

Fig. 5. SEM top-view images of TiO_2 nanotube layer formed on Ti substrate
(a) Ti-10Zr (b) Ti-20Zr (c) Ti-30Zr (d) Ti-40Zr

But, for Zr content of 10wt% (Fig. 5a), the interspace of TiO_2 nanotubes was very small, 60nm. As the Zr content increased, the interspace of TiO_2 nanotubes increased 70, 100 and 130 nm, respectively (Fig. 6).Diameter of nanotube was not depended on Zr content, but interspace of nanotube was predominantly depended on Zr content. It is confirmed that, ZrO_2 oxides play a role to formation on the surface.

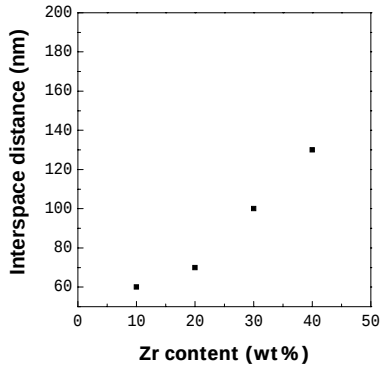

Fig. 6. Relation between the Zr content and the interspace of TiO_2 nanotubes under the same magnifications as for Fig. 5.

3.3 Electrochemcial characteristics

Fig. 7 shows the results of potentiodynamic test (potential range of -1500 ~ 2000mV) in NaCl solution, which was conducted in order to investigate the effect of Zr content on the polarization curve. It can be seen in Fig. 7(a) that the Ti-40Zr alloy has the highest resistance to corrosion. It is thought that increase of corrosion resistance with Zr content is attributed to the a few nm thick passive film such

NSTI-Nanotech 2008, www.nsti.org, ISBN 978-1-4200-8503-7 Vol. 1

as TiO_2 and ZrO_2 formed rapidly on the specimen surface. A few nm thick passive films could restrict the movement of metal ions from the metal surface to the solution, thus minimizing corrosion (Fig. 7(b)).

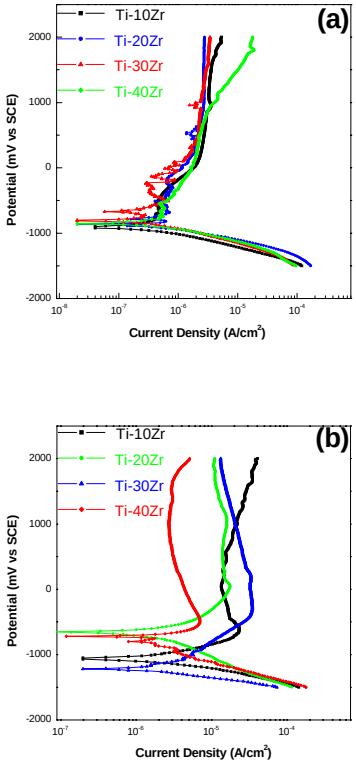

Fig.7. The polarization curves of Ti-xZr alloys after potentiodynamic test in NaCl solution at 36.5±1℃
(a) as-received (b) nanotube formed

4 CONCLUSIONS

1. Microstructure properties observed by OM and SEM changed from lamellar structure to needle-like structure with increasing Zr content.
2. Microstructure changes from β phase to α phase through XRD and α phase increases according to the amount of Zr added
3. From the results of TiO_2 nanotube layer formed in the Ti-xZr alloy, nanotubes have an inner average diameter of 150 ~ 200 nm with a tube-wall thickness of about 20nm. As the Zr content increased, the interspace of TiO_2 nanotubes increased ~60, ~70, ~100 and ~130 nm, respectively.
4. From the results of polarization behavior in the Ti-xZr alloys, the current density of nanoformed Ti-40Zr in the passive region was higher than that of other alloys.

ACKNOWLEDGEMENT

"This work was supported by research funds from Chosun University (2007) and 2nd stage of Brain Korea 21 for College of Dentistry"

REFERENCES

[1] M. Aziz-Kerrzo, KG. Conroy, AM. Fenelon, ST. Farrell, CB. Breslin, "Electrochemical studies on the stability and corrosion resistance of titanium-based implant materials", biomaterials, 22, 1531-1539, 2001.
[2] LJ. Knob, DL. Olson, "Metals handbook corrosion", 13, 669, 1987.
[3] E. Eisenbarth, D. Velten, M. Muller, R. Thull and J. Breme, "Biocompatibility of β- stabilizing elements of titanium alloys", Biomaterials, 25, 5705-5713, 2004.
[4] M.A. Khan, R.L. Williams, D.F. Williams, "The corrosion behavior of Ti-6Al-4V, Ti-6Al-7Nb and Ti-13Nb-13Zr in protein solutions", Biomaterials, 20, 631-637, 1999.
[5] KL. Wapner, "Implications of metallic corrosion in total knee arthroplasty", Clin Orthop, 271, 12-20, 1991.
[6] J. J. Park, H. C. Choe, Y. M. Ko, "Corrosion Characteristics of TiN and ZrN coated Ti-Nb alloy by RF-sputtering", Materials Science Forum, 539-543, 1270-1275, 2007.
[7] D. Kuroda, M. Ninomi, M. Morigana, Y. Kato, T. Yashiro, "Design and mechanical properties of new β type titanium alloys for implant materials", Materials Science and Engineering A, 243, 244-249, 1998.
[8] Yang BC, Uchida M, Kim HM, Zhang XD, Kokubo T, "Preparation of bioactive titanium metal via anodic oxidation treatment", Biomaterials, 25, 1003-1010, 2004.
[9] Dyer CK, Leach JSL, "Breakdown and efficency of anodic oxide grown on titanium. J. Electrochem. Soc., 125, 1032-1038, 1978
[10] marchenoir JJC, Loup JP, Masson JE, "Etude des couches poreuses formees par oxidation anodique du titane sous fortes tensions", Thin Solid Films, 66, 357-369, 1980.
[11] Zwilling V, Aucouturier M, Darque-Ceretti E, Boutry-Forveille A, "Anodic oxidation of titanium and TA6V alloy in chromic media, An electrochemical approach", Electrochemical Acta, 45, 921-929, 1999.
[12] Gong D, Grimes CA, Varghese OK, Chen Z, Dickey EC, "Titanium oxide nanotube arrays prepared by anodic oxidation, J. Mater. Res., 16, 3331-3334, 2001.
[13] A. V. Dobromyslove, V. A. Elkin, Scripta Materialia, "Martensitic transformation and metastable β-phase in binary titanium alloys with d-metals of 4-6 periods", 44, 905-910, 2001.